



Citation for published version:

Egesa, D, Chuck, CJ & Plucinski, P 2018, 'Multifunctional Role of Magnetic Nanoparticles in Efficient Microalgae Separation and Catalytic Hydrothermal Liquefaction', ACS Sustainable Chemistry and Engineering, vol. 6, no. 1, pp. 991-999. <https://doi.org/10.1021/acssuschemeng.7b03328>

DOI:

[10.1021/acssuschemeng.7b03328](https://doi.org/10.1021/acssuschemeng.7b03328)

Publication date:

2018

Document Version

Peer reviewed version

[Link to publication](#)

This document is the Accepted Manuscript version of a Published Work that appeared in final form in ACS Sustainable Chemistry and Engineering, copyright (C) American Chemical Society after peer review and technical editing by the publisher. To access the final edited and published work see <https://dx.doi.org/10.1021/acssuschemeng.7b03328>

University of Bath

General rights

Copyright and moral rights for the publications made accessible in the public portal are retained by the authors and/or other copyright owners and it is a condition of accessing publications that users recognise and abide by the legal requirements associated with these rights.

Take down policy

If you believe that this document breaches copyright please contact us providing details, and we will remove access to the work immediately and investigate your claim.

Multifunctional Role of Magnetic Nanoparticles in Efficient Microalgae Separation and Catalytic Hydrothermal Liquefaction

Daniel Egesa, Christopher J. Chuck, Pawel Plucinski*

Center for Sustainable Chemical Technology, Department of Chemical Engineering, University of Bath, Claverton Down, Bath, BA2 7AY, United Kingdom. Email: P.Plucinski@bath.ac.uk

Supporting Information

ABSTRACT: In this work, the efficiency of extracting algae from culture medium using magnetic nanoparticles (MNPs), converting the algal/particle slurry to bio-crude using hydrothermal liquefaction (HTL) and successfully recycling the MNPs from the char phase was fully demonstrated for the first time. MNPs were synthesized by co-precipitation and used to extract algae from aqueous phase at a separation efficiency (SE) of 99%. The SE was optimized at pH 4. Liquefaction of algal/MNPs slurry gave a bio-crude yield of 37.1% while algae only yielded 23.2%. The percentage area in the GC-MS chromatogram corresponding to hydrocarbons (HC) in Zn-ferrite catalyzed and uncatalyzed bio-crude was 46.5% and 19.9% respectively while the percentage area of heptadecane from Zn-ferrite catalyzed and uncatalyzed bio-crude was 37.8% and 10% respectively. Furthermore, the percentage area of hetero atom compounds in bio-crude reduced substantially when liquefaction was done in presence of Zn and Mg ferrites. The nanoparticles were recovered from biochar by sonication and recycled at a SE of 96.1%. Recycling of MNPs for magnetic separation of algae and catalytic HTL could lower the cost of microalgae harvesting and improve the yield and quality of bio-crude. This could potentially reduce the cost of advanced biofuel processing from microalgae making them more affordable in comparison to petroleum derived fuels.

KEYWORDS: Magnetic separation, magnetic nanoparticles, separation efficiency, hydrothermal liquefaction, bio-crude, recycling

INTRODUCTION

The irreversible depletion of fossil fuels and resulting environmental impact from their use has encouraged research into alternative sources of renewable liquid fuels.¹ Currently, most biofuels are produced from first generation feedstocks such as sugarcane, soybean and corn. This is disadvantageous mainly due to competition between fuel and food for the limited food sources. While some non-food sources such as *Jatropha* are an improvement, these too have disadvantages *e.g.* competition for good quality agricultural land with food crops.² One promising alternative is microalgae because of their high productivity, they can be cultivated on large water bodies, with low quality water³ therefore potentially do not compete for fertile agricultural land hence minimal environmental impact on good agricultural land.^{4,5}

However, one of the major limitations of processing biofuels from microalgae is the high cost of microalgae harvesting (separation) which contributes up to 25% of the overall cost of biomass processing.⁶ This is in part due to difficult cell separation because of a slow settling velocity of microalgae due to their small size, low concentration and the resulting repulsion between the negatively charged cells.⁷ Generally methods currently used to harvest microalgae are extremely slow or expensive and energy intensive.⁸ A promising alternative is magnetic separation of microalgae because it is easy to manipulate and regenerate, it uses simple devices, it is cost effective and the magnetic field is nondestructive and economical.^{9,10,11} It was also reported on Los Alamos web site,¹² that magnetic separation can reduce the cost of algae harvesting by 90%.

Magnetic separations rely on adsorption of charged magnetic nanoparticles onto microalgae cells which then respond to an external magnetic field concentrating the algal cells.

In this work, microalgae were separated magnetically and subjected to hydrothermal liquefaction (HTL) to produce bio-crude oils. The HTL process entails using water as a reactive medium to convert biomass into liquid crude oil under controlled conditions. In this conversion, the main cellular constituents such as lipids, proteins and carbohydrates are broken down at the high temperatures and pressures. This coupled with hydrolytic attack leads to breakage of biomolecules in hot compressed water resulting into the production of a bio-crude oil,¹² with a reasonably high calorific value.¹³ This process uses the whole algae cell and does not require the algae to over produce lipid, allowing the use of faster, denser growing strains. Due to the difficulties of cultivating lipid rich algae and extracting these lipids from microalgae cells, the HTL process is considered as a more viable alternative to produce a biofuel product from microalgae.^{2,13} Life cycle and techno economic analysis suggests that the overall HTL process uses less energy than the extraction and transesterification of lipids,¹⁴ though further work is required to increase bio-crude yields and quality. To this end, effort has been invested in investigating the effect of catalysts on the HTL process and its ability to produce higher quality products.¹⁶

Among heterogeneous catalysts, solid nano-catalysts have attracted a lot of attention due to their large chemically active surface area and high chemical and physical stability which are important factors in industrial applications.¹⁶ One of the key challenges with

solid catalysts is in their recovery from the catalyst bio-crude mixture by means of filtration methods which are generally not economically viable. Therefore it is paramount to develop heterogeneous catalysts that can easily be recovered and recycled for continuous HTL reactions.¹⁷ Magnetite based nano-catalysts are interesting potential candidates because they can easily be separated by magnetic force hence improving their lifetime and cost effectiveness. Also, they have large specific surface areas, less resistance to mass transfer and high catalytic activity for bio catalysis, photo catalysis, and phase transfer catalysis.¹⁷ No study has yet demonstrated the multifunctional role of magnetite based nano-catalysts in HTL and microalgae separation however.

The aim of this research is to potentially lower the processing cost of biofuel from microalgae by optimising microalgae separation efficiency and improving yield and quality of bio-crude from algae HTL. The objectives are: (i) to magnetically separate microalgae from culture medium at a separation efficiency above 95%, (ii) to investigate the catalytic effect of doped MNPs on yield and chemical composition of bio-crude and (iii) to recycle MNPs for magnetic separation and HTL catalysis. To our knowledge, this is the first time MNPs have been used to play a dual role: harvesting microalgae and catalysing the HTL process. It will also be the first report on recycling MNPs from HTL to further harvest microalgae and catalyse HTL process. Achieving the above objectives could lead to a cost-effective processing of biofuels from microalgae resulting into biofuels being more economically competitive with petroleum derived fuels. As well as a more sustainable approach to bio-crude processing since MNPs are easily recycled minimising waste.

MATERIALS AND METHODS

Synthesis of MNPs and Magnetic Separation of *S. Obliquus*

Ferrite magnetic nanoparticles (MNPs) were synthesized by coprecipitation method.^{18,19} They were then used to separate microalgae from culture medium and separation efficiency (SE) was optimised at different pH and mass ratios of MNPs: microalgae. SE was calculated according to equation 1.²⁰

$$SE = \frac{OB-OA}{OB} \times 100 (\%) \quad (1)$$

Where: *SE* is the separation efficiency, *OB* is optical density before separation, *OA* is optical density after separation. *Scenedesmus obliquus* was grown in illuminated photo-bioreactors supplied with CO₂ at pH 8 and temperature 25°C. *Spirulina* was purchased from Bulk Powders® and was composed of 63% protein, 20% carbohydrates 6% fat and 11% miscellaneous biochemical content. Details of materials and methods of synthesizing MNPs, magnetic separation and algae culture composition are in the supporting information (SI).

Hydrothermal Liquefaction of microalgae

After magnetic separation, microalgae/MNPs slurry was subjected to HTL at 320°C for 1 hour according to the method reported by Coma *et al.*²¹ MNPs were recovered from the solid residue by sonication in de-oxygenated and de-ionized water to remove any attached bio-mass and then magnetically extracted from the water. Details of HTL procedure and MNP recovery can be found in the SI. All experiments were repeated twice. The corresponding values of standard deviation can be found in Figures and Tables.

Bio-crude Oil Analysis

The percentage yield of HTL products (bio-crude and solid residue) was calculated using equation 2.²² The mass of MNPs was subtracted from the solid residue and the yield of bio-crude and solid residue was calculated on an ash and moisture free weight basis using equation 2 below.

$$YP = \frac{WP}{WF-WA-WM} \times 100 (\%) \quad (2)$$

Where, *YP* is the percentage yield of the product, *WP* is the mass of product (g), *WF* is mass of microalgae fed into the reactor, *WA* and *WM* are ash and moisture content of microalgae. The ash content for the dried *Spirulina* and *S.obliquus* varied between 16% to 18% and 22% to 25% and the moisture content was between 8% to 10% and 10% to 12% respectively. The high heating value (HHV) of bio-crude was determined using Dulong's formula.¹³ The energy recovery (ER) for the bio-crude was calculated according to equation 3:²²

$$ER = \frac{(HHV_p \times Oil\ Yield)}{(HHV_f)} \times 100 (\%) \quad (3)$$

Where: *ER* is the energy recovery, *HHV_p* is high heating value of product, and *HHV_f* is high heating value of feed.

Analytical Techniques

Optical density measurements were done using a UV-Vis Cary series instrument JEM-1200 EX11. Surface morphology and size of MNPs was analysed using a JEM-1200 EX11 TEM instrument at an acceleration voltage of 300kV. The size distribution of MNPs was determined using image J software. The surface morphology of microalgae cells and the attached MNPs was done on a JEOL JSM 6330F FE-SEM equipment at an acceleration voltage of 2.5kV. The crystal structure and phase composition of MNPs was characterized on a Bruker D8 Advanced XRD machine operating at 40 kV and 80 mA and a scanning rate of 0.02°/s in 2θ range from 20° to 70°. Compounds in the bio-crude were analysed by GC-MS on an Agilent technologies GC system 7890A with triple axis detector, 5975 network mass selective detector and Agilent JW scientific GC column. Moisture and ash content of microalgae biomass was determined through TGA analysis. TGA runs were done on a TGA 92 Setram equipment. ¹HNMR analysis of bio-crude was done on a 400 MHz Bruker NMR machine. Elemental composition of bio-crude was done in duplicate using a Carlo Erba Flash 2000 elemental analyser.

RESULTS AND DISCUSSION

Synthesis and Characterization of MNPs

TEM images (Figure S2A) show that magnetite nanoparticles were crystalline, mono dispersed and mostly in the size range of 10-12 nm. The particle size was measured using image J software. Doped MNPs (ferrites) were poly-dispersed with increased particle size mostly ranging between 16 to 18 nm (Figures S2 B, C and D). The increase in particle size with doping is confirmed by XRD results (Figures S4 A, B and C) which show increased intensity and sharpening of peaks with doping. The sharpening of peaks is an indication of increased particle size as a result of doping with Zn and Mg.²³ Reflections which correspond to magnetite nanoparticles were found at 2θ = 30.437°, 35.715°, 43.393°, 53.950° and 57.309° corresponding to the (220), (311), (400), (422), and (511) crystal planes of pure magnetite. These peaks match well with the reported

peaks in literature for magnetite.²⁴ The sharpest peaks were from Zn and Mg doped magnetite nanoparticles with the highest (311) at Lin count of 4700, the less intense peaks were for un-doped Fe₃O₄ (311) at 1150 Lin count. Formation of magnetite nanoparticles was also monitored by UV-Vis (Figure S5). From the UV-Vis spectrum hydrolysis of iron ions in presence of ammonium hydroxide resulted into removal of metal-ion complex from solution leading to the disappearance of the peak at 300 nm and to formation of a second broad featureless absorption tail which according to Melo *et al.*²⁵ is due to formation of magnetite and is as a result of transition in band gap of semiconductor materials.

Magnetic separation of microalgae

The separation efficiency (SE) of *Scenedesmus obliquus* was optimised at different separation times, pH and mass ratios of MNPs to *S. obliquus*. Microalgae SE increased with an increase in separation time (Figure 1). SE also increased with increase in mass ratio of MNPs to microalgae (Figure 2). This trend is in agreement with the findings of Prochazkova *et al.*^{9,20} in separation of *C. vulgaris* where 90% separation was achieved. Cerff *et al.*²⁶ also observed a similar trend while separating fresh water microalgae *C. reinhardtii* and *C. vulgaris*. The increase in SE with mass ratio is attributed to presence of more nanoparticles to adsorb onto the microalgae surface resulting in increased magnetic force and a higher SE. The higher the concentration of MNPs, the greater the adsorption hence the stronger the magnetic force resulting in faster separation. Further increase in the concentration of MNPs had no effect on SE. This is presumably because magnetic force is proportional to the volume of the magnetic body, if the volume of the MNPs increases, the magnetic force increases resulting in a better separation. Cells with much less or no MNPs adsorbed will not respond to magnetic force.

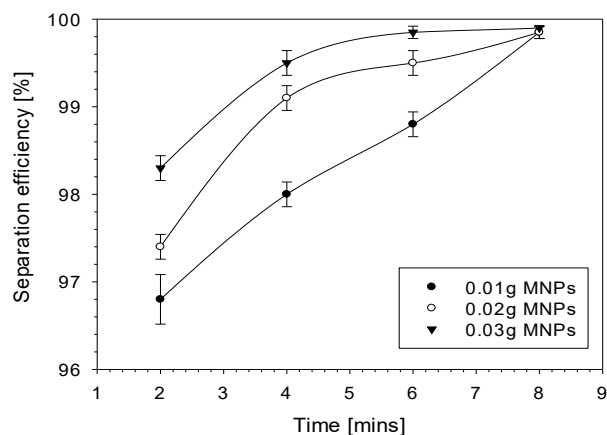


Figure 1. Separation efficiency of *Scenedesmus obliquus* (0.5g/L, 20 ml, pH4) at varying time intervals and mass ratios of magnetite.

The high SE in acidic pH is attributed to a highly-pronounced difference in ζ -potential (ZP) measurements of the interacting particles.^{6,9} The difference in ZP was highest at pH4 (49 mV) and lowest at pH 11(27.9 mV). Micro-algal cells maintain a negative surface charge over a wide pH range and in acidic pH below the isoelectric point, the surface charge of MNPs is positive because they gain protons.^{6,28} Therefore, there is a higher electrostatic attraction between positively charged MNPs and negatively charged micro-algal cells. The difference in ZP of MNPs and micro-algal cells was more pronounced in acidic pH (Figure S6). This led to greater interaction between MNPs and microalgae cells hence a higher SE. The low SE at basic pH is as a result of MNPs gaining electrons above its isoelectric point and hence become negatively charged.⁶

²⁸ This results in repulsion between algae and MNPs hence a lower SE. The limited separation that takes place is due to the attachment between MNPs and microalgae cells at molecular level brought about by restricted electron interactions and positively charged sections within the suspension.^{6,29}

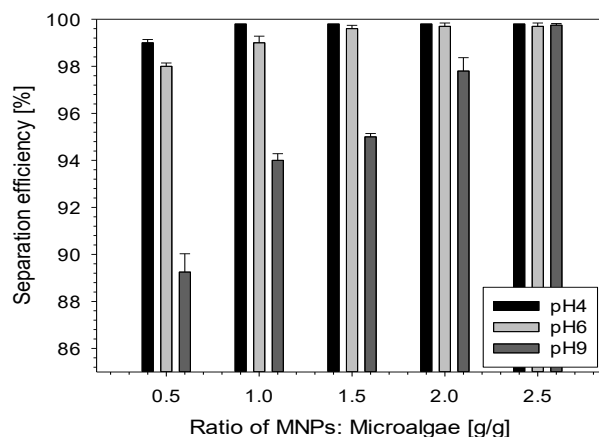


Figure 2. Separation efficiency of *Scenedesmus obliquus* (0.5 g/L, 20 ml, separation time 4 minutes) at different mass ratios and pH.

Catalytic effect of MNPs on bio-crude yield in HTL

The extraction of the microalgae using MNPs leaves an algal/MNPs slurry with a water content of 78%. This is directly in the range for HTL processing. The effect of the MNPs on the bio-crude yield was therefore examined at different mass ratios of MNPs to microalgae (Figure 3A) using both *Spirulina* and *S. obliquus* strains. Excitingly, bio-crude yields were increased substantially on addition of MNPs, with the highest yield (34%) achieved at a ratio of 0.12, this is in comparison to only 25% when using *Spirulina* alone. A number of other studies have demonstrated an increase in yield on using metal catalysts.¹³ The further increase in mass of MNPs did not have any substantial effect on yield. This nonlinear correlation between catalyst loading and bio-crude yield has also been reported by Rojas *et al.*¹³ while investigating the catalytic effect of magnetite nanoparticles on macro-algae bio-crude production. Also, studies on coal liquefaction by Dadyburjor *et al.*³⁰ found that optimum yields were obtained at low iron oxide catalyst ratios. The high bio-crude yield at an optimum loading of MNPs can be attributed to an effective distribution of MNPs (catalyst) on the surface of the algae cells (see Figure S11D) resulting into maximum exposure of active sites which facilitate increased conversion of algal biomass to bio-crude. Additionally, the low yield at higher particle loading can be attributed to increased particle aggregation seen at the algal cell surface (Figure S11F). This results in loss of catalyst due to a reduction in accessible active sites hence reduced conversion of algal biomass to bio-crude. These results show that the yield of bio-crude in HTL can be enhanced by an optimum quantity of MNPs.

The yield of the solid residue was lower when *Spirulina* liquefaction was done in presence of MNPs (Figure 3A). The reduction in solid residue yield has been confirmed by elemental analysis (Table S3) showing reduction in carbon content of the residue for runs involving MNPs. The reduction in solid residue in presence of MNPs can be attributed to their catalytic effect in favouring the conversion of algae biomass into bio-crude.

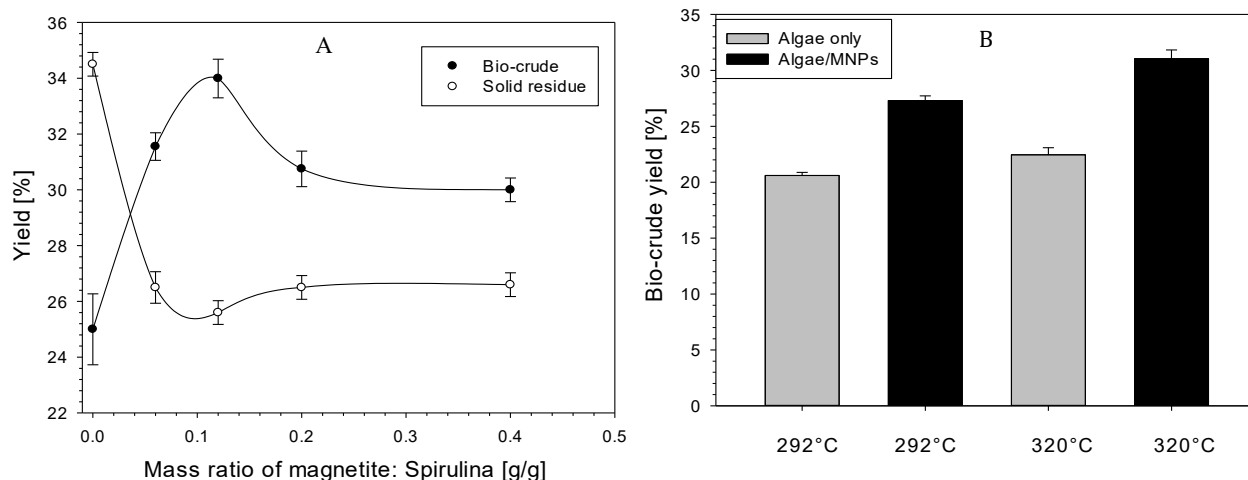


Figure 3. Bio-crude yield from microalgae HTL with and without magnetite at 320°C, P₀ of 50 bar (N₂) and P₁ of 120 bar for 60 minutes, A) Yield from HTL of Spirulina at different mass ratios of magnetite to Spirulina. B) Yield of bio-crude from HTL of *Scenedesmus obliquus* (mass ratio of magnetite: algae of 0.4 g/g).

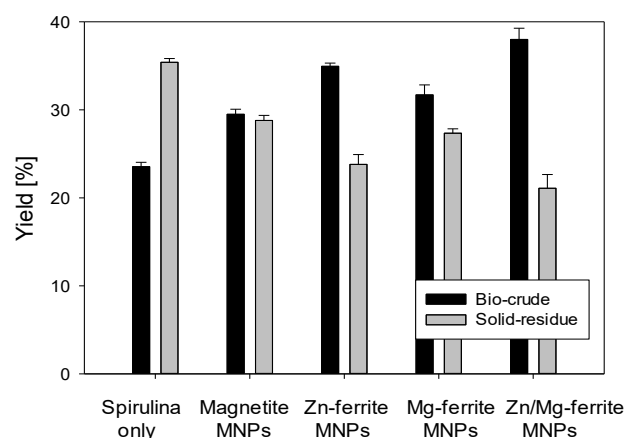


Figure 4. Yield of bio-crude and solid residue from HTL of Spirulina biomass in presence of different doped MNPs at 320°C, for 60 minutes at a mass ratio of MNPs: Spirulina of 0.12 g/g.

Liquefaction in absence of MNPs resulted in a higher yield of solid residue (34.5%) which was translated into a lower yield of bio-crude. It seems clear therefore that MNPs are having a catalytic effect on the conversion of the microalgae, favouring bio-crude production and reduced solid residue. The detailed catalytic mechanism needs further investigation since the HTL process involves many different reactions. Furthermore, in liquefaction of *S. obliquus* (Figure 3B) the presence of MNPs had a similar effect on bio-crude yield. The highest bio-crude yield of 30.5% was observed at 320°C in presence of magnetite while in absence a bio-crude yield of 22% was achieved. All bio-crude yields reported greatly exceed the lipid content of the original feed stock. This confirms that other cellular components like proteins and carbohydrates were also converted during the HTL process.²

Zn and Mg doped ferrite MNPs had an even larger impact on the liquefaction of Spirulina biomass. Doped ferrite MNPs greatly enhanced the yield of bio-crude compared to pure magnetite (Figure 4). The highest yield (37.1%) was observed when Zn/Mg/Fe₃O₄

was used giving a 14% increment in yield in comparison to liquefaction without nanoparticles and an 8% increment in yield compared to pure magnetite. Also, Zn doped ferrite registered a bio-crude increment of 11.5% compared to liquefaction without MNPs. Doped MNPs also had a substantial effect on reducing the percentage of ash free solid residue, the largest reduction (15.7%) was observed when Zn/Mg/ferrite was used (Figure 4). Liquefaction without MNPs resulted into a higher percentage of solid residue (35.7), this is reflected in the reduced yield of the bio-crude (23.2%). Similar increases in yield were observed when Mg, Zn, and Fe sulphates were present in the liquefaction of spirulina.³¹

This suggests that the use of MNPs can be applied to a range of algal species and a similar increase in HTL yields can be expected. By doping with either Mg or Zn further gains can be made in the bio-crude yield. The MNPs play two important roles: separation of microalgae from the culture medium and a catalytic role of increasing the yield of bio-crude during the HTL.

Effect of MNPs on Chemical Composition of the bio-crude

To determine the catalytic effect of MNPs on the chemical composition of the bio-crude elemental analysis, GCMS and NMR analyses were performed.

Elemental composition

The elemental composition of bio-crude from Spirulina liquefaction were compared at different mass ratios of MNPs: microalgae and when using different doped ferrite MNPs (Table1). The amount of carbon and hydrogen in the bio-crude was much higher than that in the biomass feedstock. The carbon content of the bio-crude increased from 46.3% in Spirulina feedstock to 71.9% in un-catalysed bio-crude and to 73% in catalysed bio-crude while the hydrogen content increased from 6.6% in Spirulina feed stock to 9.2% in un-catalysed liquefaction. Increasing concentration of MNPs did not have a significant impact on the carbon and hydrogen content of the bio-crude. The highest carbon content (73%) was achieved at a mass ratio of 0.12. This was the most optimum loading of MNPs for the highest possible yield of carbon. This trend is in agreement with the findings of Raikova *et al.*³¹ on the effect of metal sulphates on Spirulina liquefaction. A similar range in carbon

Table 1. Elemental compositions, HHV, atomic ratios and ER of Spirulina and bio-crudes from spirulina liquefaction at different masse ratios of magnetite: microalgae and using different ferrite MNPs. HTL was done at 320°C for 60 minutes, at P₀ of 50 bar (N₂), and P_f of 120 bar.

Ratio Fe ₃ O ₄ : algae	C (wt %)	H (wt %)	N (wt %)	O (wt %)	S (wt %)	N/C*	H/C*	O/C*	HHV (MJ/kg)	ER (%)
Spirulina	46.3±0.06	6.65±0.00	10.3±0.06	27.7±0.03	0.54±0.01	0.19	1.72	0.45	20.3±0.4	0.00
0	71.9±0.06	9.24±0.04	7.50±0.11	10.0±0.04	0.41±0.03	0.09	1.54	0.10	35.7±0.2	44.0±2.24
0.06	71.9±0.11	8.8±0.120	6.60±0.09	9.4±0.04	0.60±0.03	0.08	1.47	0.10	35.3±0.1	54.9±0.86
0.12	73.0±0.04	9.09±0.09	7.40±0.06	9.4±0.01	0.77±0.03	0.09	1.49	0.10	36.2±0.2	60.8±1.24
0.2	69.3±0.1	8.56±0.06	6.05±0.11	9.8±0.01	0.50±0.02	0.07	1.48	0.14	34.0±0.1	51.5±1.07
0.6	70.7±0.08	8.69±0.05	6.54±0.07	10.7±0.1	0.69±0.00	0.08	1.47	0.11	34.5±0.2	51.0±0.72
Type of MNPs										
Spirulina	46.3±0.06	6.65±0.00	10.3±0.06	27.7±0.03	0.54±0.01	0.23	0.14±0.00	0.60	20.3±0.03	0.00
No MNPs	71.9±0.06	9.24±0.04	7.5±0.11	10.0±0.04	0.41±0.03	0.10	0.13	0.14	35.7±0.03	40.9±0.1
Magnetite	72.6±0.04	9.20±0.09	7.20±0.06	9.40±0.01	0.77±0.03	0.10	0.13	0.13	36.1±0.15	51.7±0.2
Mg ferrite	73.0±0.06	8.64±0.04	7.41±0.01	9.56±0.05	0.53±0.02	0.10	0.12	0.13	35.4±0.03	53.8±0.1
Zn ferrite	72.1±0.15	8.75±0.00	7.58±0.02	10.2±0.00	0.60±0.00	0.11	0.12	0.14	35.1±0.05	60.0±0.1
Mg/Zn ferrite	72.9±0.09	8.74±0.01	7.07±0.04	9.71±0.02	0.60±0.01	0.10	0.12	0.13	35.4±0.05	64.8±0.1

* Molar ratios

and hydrogen contents was observed when liquefaction of microalgae was done in presence of Zn and Mg doped ferrite MNPs. Therefore, HTL of micro-algae in the presence of MNPs leads to increment in the carbon content of bio-crude. The amount of oxygen and nitrogen in the biomass feedstock was also much higher than that in the bio-crude. The oxygen content in the bio-crude was reduced from 27.7% in the biomass feedstock to 10% in bio-crude from un-catalysed liquefaction and to 9.4% in bio oils from catalysed liquefaction (Table 1). Oxygen reduction coupled with an increase in amount of carbon and hydrogen resulted in bio-crude having a higher energy density than the microalgae feed stock. The nitrogen content in the bio-crude was reduced from 10.3% in the biomass feedstock to 7.5% in bio-crude from un-catalysed liquefaction and to 6% in bio-crude from catalysed liquefaction. The further reduction in oxygen and nitrogen content of bio-crudes in the catalysed liquefaction shows that the presence of MNPs played a major role in de-oxygenation and de-nitrogenation of the bio-crude and can potentially be used as HTL catalysts to improve the quality of the bio-crudes.

Liquefaction in the presence of MNPs led to the highest energy recovery (ER) value of 60.8% at a mass ratio of 0.12 giving an increment of 10.9% in comparison with bio-crude from the un-catalysed liquefaction. The high ER at this concentration corresponds well with the high heating value (HHV) at the same concentration. The highest ER was achieved when liquefaction was done in presence of Mg and Zn doped ferrite MNPs. This gave a percentage increment of 23.9% in comparison with the bio-crude from the un-catalysed liquefaction. Zn ferrites also gave a high ER of 60%. This shows that Zn and Mg doped ferrite MNPs have a large influence on increasing the ER of the bio-crudes.

GC-MS Analysis of Bio-crude

The identities of the main individual compounds (extracted by hexadecane) in the bio-crude from *Spirulina* and *Scenedesmus obliquus* liquefaction (Figure 5) and their relative percentage areas in the chromatogram after integration were determined. Peaks in the chromatogram with less than 1% relative area were not considered. The major compounds detected in the bio-crude were grouped under hydrocarbons, aromatic hydrocarbons, nitrogen compounds, phenolic compounds, oxygenated compounds, and organic acids. The hydrocarbons (HC) grouping consisted of compounds such as octane, cyclohexane, cyclopropane, hexadecane, heptadecane, and nonyne. In Figure 5, bio-crude from un-catalysed liquefaction registered the lowest percentage area of hydrocarbons (19.9%) while bio-crude produced in presence of Zn ferrite MNPs registered the highest percentage area (46.5%). Liquefaction in the presence of Mg and Zn ferrite MNPs also gave a high percentage area of HC (36%).

The increase in hydrocarbon composition in the presence of Zn and Mg ferrite MNPs is an indication of their catalytic role in promoting decomposition of cellular components like lipids, proteins and carbohydrates and the ability to produce hydrocarbons.² The hydrocarbons from both bio-crudes were largely composed of alkanes with heptadecane as the most predominant. A high percentage of heptadecane (37.8%) was observed when liquefaction of *Spirulina* was done in presence of Zn ferrite MNPs. Liquefaction of *Spirulina* in absence of MNPs registered a low percentage (10%) of heptadecane in the bio-crude. For *Scenedesmus obliquus* bio-crude (Figure 5B), the percentage of heptadecane in the bio-crude was 20% when

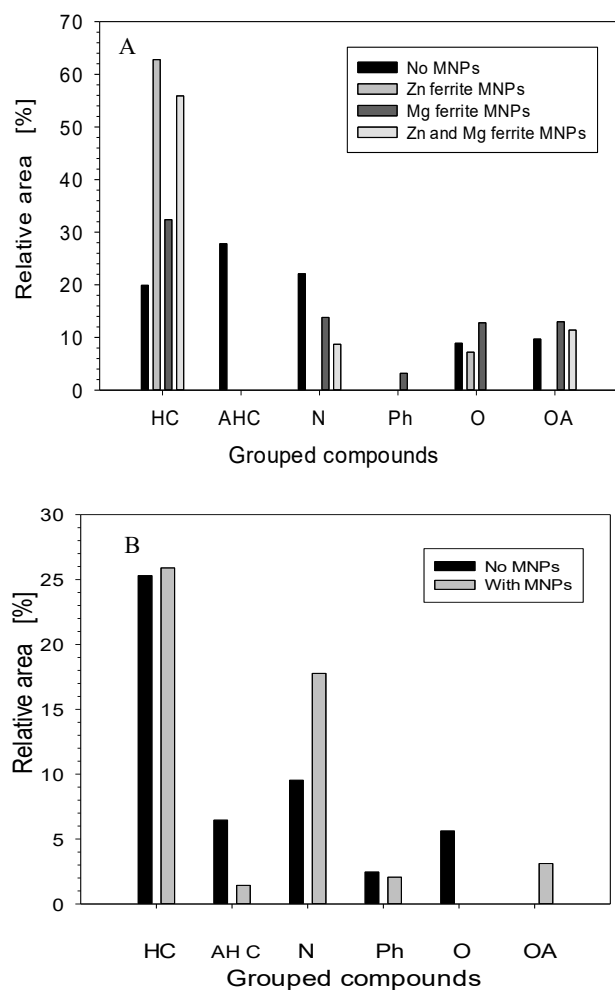


Figure 5. Distribution of major compounds in bio-crude after microalgae HTL at 320°C at P_0 of 50 bar (N_2), P_f 120 bar for 60 minutes at ratio of MNPs: algae 0.12 g/g: A) Spirulina in presence of different MNPs and B), *S. obliquus* in presence of magnetite. HC – hydrocarbons, AHC – aromatic hydrocarbons, N – nitrogen compounds, Ph – phenolics, O – oxygenates, OA – organic acids.

liquefaction was done in presence of magnetite and 3.1% when liquefaction was done in absence of magnetite. These results suggest that the catalysts are aiding the deoxygenation of lipids and fatty acids into the hydrocarbon species more effectively than the non-catalysed process. Interestingly, there were more aromatic hydrocarbons (AH) in bio-crude from un-catalysed liquefaction. Liquefaction of *Scenedesmus obliquus* in the presence of magnetite led to reduction in AH by 5.03% while liquefaction of Spirulina in the presence of MNPs led to a 26.8% reduction in AH. This shows that HTL in presence of MNPs facilitated the catalytic conversion of AH to other compounds within the bio-crude.

The grouping of nitrogen compounds included: cyclo-heptylamine, indole, acetamide, 3-pyridinecarbonitrile, butanamide, NN-dimethyl decanamide, isobutyl isothiocyanate, azetidine, benzonitrile and pyrimidine. The un-catalysed bio-crude from Spirulina contained more nitrogen compounds (22.1%) compared to *Scenedesmus obliquus* bio-crude (9.5%). The high percentage of nitrogen compounds in Spirulina bio-crude is attributed to its high protein content (63%). The proteins undergo degradation through different reaction pathways such as deamination, decarboxylation, dehydration, and depolymerisation to form nitrogen compounds.³²

³⁰ The amino acids from proteins undergo decarboxylation and deamination reactions to form amines, ammonia, carbonic acids, and other organic compounds.^{32, 34} In Spirulina bio-crude, the amount of nitrogen compounds reduced to below 1% after liquefaction with Zn ferrite MNPs while liquefaction with Zn/Mg ferrite led to a decrease of 13.4%. This trend has also been reported by Biller *et al.* when liquefying different microalgae species in presence of sodium carbonate catalyst. Elemental analysis results also show a general reduction in the percentage of elemental N in catalysed bio-crude. This confirms that Zn and Mg doped ferrite MNPs play a catalytic role in removing nitrogen compounds from bio-crude presumably producing more water-soluble species hence improving the bio-crude quality.

The grouping of phenolic compounds had only phenol and it was observed in significant quantities in the bio-crude from *Scenedesmus obliquus*. The amount of phenol in un-catalysed bio-crude was slightly higher than that in catalysed. The percentage of phenol in un-catalysed and catalysed bio-crude from Spirulina liquefaction was below detachable levels only bio-crude from Mg ferrite liquefaction (Figure 5A) had a percentage of phenolic compounds of up to 3.2%. A similar trend was observed by Rajdeep *et al.* in microalgal liquefaction at 250°C. Since microalgae bio-crudes do not possess lignin it is possible that phenolic compounds were produced from carbohydrates within the algal biomass^{2, 29} having been hydrolysed to glucose which is broken down to furfural and finally condensed to phenols.^{32, 35} The other grouping included compounds such as propanal and cyclopentan-1-one belonging to aldehydes, ketones and esters. These were grouped under oxygenated compounds. The un-catalysed bio-crude from *S. obliquus* had significant quantities of oxygenates (5.6%). However, the bio-crude from catalysed *S. obliquus* did not show oxygenates. For Spirulina, the un-catalysed bio-crude had more oxygenates (8.9%) than the un-catalysed *S. obliquus*. Spirulina biomass liquefied in presence of Zn and Mg ferrite did not show any oxygenates. This is in agreement with elemental analysis results which revealed a reduction in oxygen when microalgae liquefaction was done in presence of MNPs. Hence confirming that Zn and Mg ferrite MNPs played a catalytic role in deoxygenation of bio-crude.

The grouping of organic acids included compounds such as n-hexa-decanoic acid, formic acid, 4-butyl benzoic acid, and propyl phosphonic acid. Liquefaction of *S. obliquus* in presence of ferrite MNPs resulted into increase in organic acids from below 1% in un-catalysed liquefaction to 3.1% in catalysed liquefaction. The organic acids were predominantly n-hexadecanoic acid (3.1%). For bio-crude from Spirulina liquefaction the amount of organic acids increased by 3.3% in Mg ferrite catalysed bio-crude. Hydrolysis of fats in microalgae biomass led to formation of fatty acids and fatty acid esters in bio-crude.^{2, 32} Due to the low concentration of tri-glycerides in microalgae biomass, fatty acids in the bio-crude may have also arisen from other pathways such as from breakdown of glucose under HTL conditions leading to formation of organic acids such as formic acid, acetic acid, lactic acid *etc.*^{32, 36} The reduction in the amount of organic acids in Zn ferrite catalysed bio-crude was possible due to their catalytic effect in breaking down fatty acids to hydrocarbons as confirmed by the highest yield of hydrocarbons in bio-crude from Zn ferrite catalysed liquefaction (Figure 5A).

NMR Analysis of Bio-Crude

To further confirm the identity and quantity of functional groups in the bio-crudes, the samples were analysed by ¹H NMR. All signals relating to the protons in the bio-crudes were grouped (Figure 6).

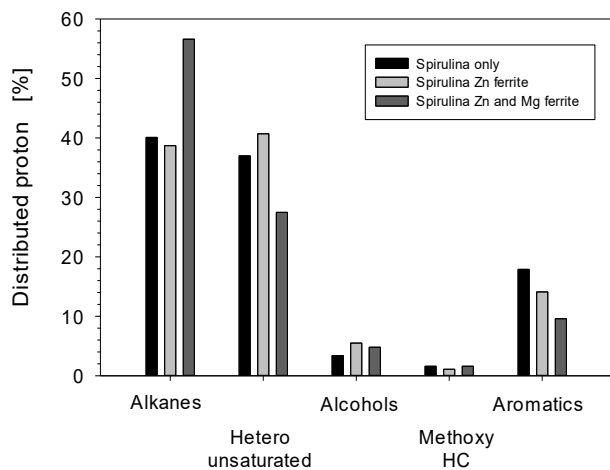


Figure 6. Grouped compounds in ^1H NMR spectrum of bio-crude from *Spirulina* liquefied with and without MNPs, liquefaction time 60 minutes at 320°C .

Large peaks were seen at 0.5 - 1.5 ppm which are characteristic of terminal methyl groups in alkyl chain corresponding to alkanes.² The ^1H NMR spectra (Figure S10) provided compatible functional group information to GC-MS chromatograph and a comparison of integrated areas in both spectra revealed a similar trend in the quantities and functional groups of corresponding compounds. Like GC-MS, ^1H NMR spectra revealed a high percentage of aliphatic functional groups corresponding to alkanes for all the bio-crudes. The high percentage of hetero/unsaturated functional groups (1.5 - 3.0 ppm) and aromatics and hetero aromatics (6.0 - 8.5 ppm) in all the bio-crudes is due to the large percentage of nitrogenous and oxygenated compounds from the feedstock's high protein (63%) content.¹⁶ Zn and Mg ferrite derived bio-crudes registered the lowest percentage of these functionalities compared to the other bio-crudes revealing a positive impact in reducing hetero/unsaturated and aromatic and hetero aromatic atom functionalities from the bio-crudes. The ^1H NMR data supports both the GC-MS and elemental analysis, demonstrating increased removal of hetero atom functionalities from bio-crudes using MNPs in HTL. Furthermore, all bio-crudes exhibited a low percentage of methoxy and carbohydrate functional groups (4.4 - 6.0 ppm), this is compatible with carbohydrates changing into bio-crude in the HTL process.²

Recycling of MNPs from HTL

After magnetic separation and HTL, MNPs largely deposited in the solid residue.

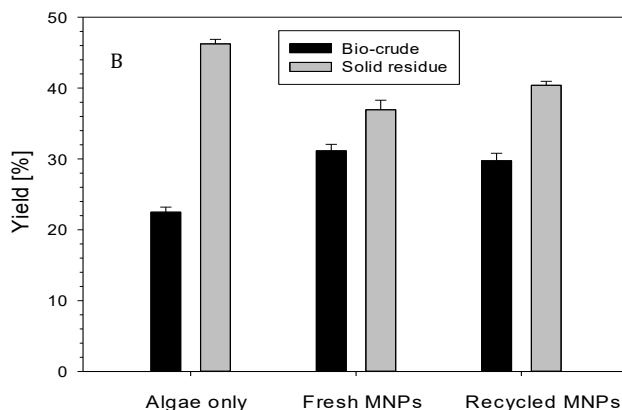
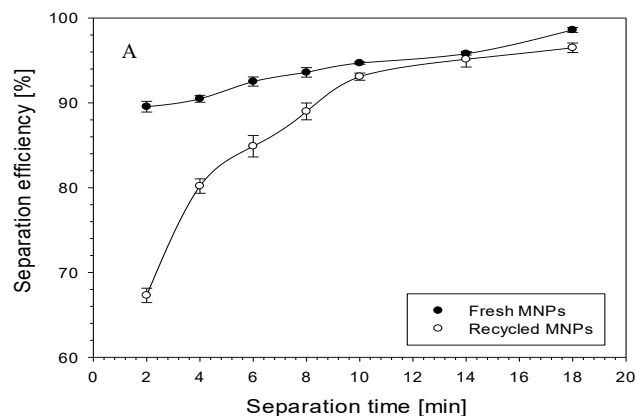


Figure 7: A) Separation efficiency of *S. obliquus* using fresh and recycled MNPs at a mass ratio of MNPs to *S. obliquus* of 0.4 g/g, pH 9.0 and separation time of 4 minutes, B) bio-crude yield from *S. obliquus* liquefaction in presence of fresh and recycled magnetite nanoparticles at 320°C for 60 minutes.

These were then recovered by sonication as described earlier. The MNPs were then tested for their suitability in harvesting further micro-algal cultures. The separation efficiency of fresh and recycled MNPs was compared at pH 9 and mass ratio of MNPs: microalgae of 0.4 g/g. After 18 minutes of separation (Figure 7A), recycled MNPs registered a SE of 96.1% compared to 98.4% for fresh ones. The microalgae/recycled MNP slurry was subjected to HTL and the yield of bio-crude from re-cycled MNPs was 29% compared to 30.5% from fresh MNPs and 22% from un-catalysed micro-algal liquefaction (Figure 7B). These results show that after the HTL process, MNPs can be recycled to efficiently harvest more microalgae and to further catalyse the HTL process. This therefore confirms that MNPs can be applied to both separate microalgae and to catalyse the HTL process hence playing two roles as microalgae harvesting agents and as HTL catalysts.

CONCLUSIONS

In this work MNPs were synthesised by co-precipitation and used to harvest microalgae at an optimised separation efficiency of 99%. The microalgae/MNPs slurry was then subjected directly to HTL process to investigate the catalytic effect of MNPs on yield and chemical composition of bio-crude. It was demonstrated that the yield of bio-crude was increased by 13.9% when HTL of microalgae was done in presence of Zn and Mg doped ferrite MNPs. When Zn doped ferrite MNPs were used in *Spirulina* liquefaction, GC-MS results revealed that the percentage area of hydrocarbons in the bio-crude increased by 26.6% and the percentage area of heptadecane increased by 27.8%. The percentage of hetero atom compounds, nitrogen and oxygen in the bio-crude were reduced when HTL was done in the presence of MNPs. This revealed that MNPs did not only play an efficient microalgae separation role but also a catalytic role. Furthermore, MNPs were easily recovered and recycled to harvest more microalgae and to further catalyse the HTL process. It was observed that recycled MNPs were still effective in magnetic separation and HTL catalysis. Using recycled MNPs, a separation efficiency of 96.1% was achieved and the bio-crude yield was increased by 7% compared to an increment of 8.7% when fresh MNPs were used in HTL.

Therefore, we have demonstrated for the first time the application of MNPs to harvest microalgae efficiently, to use these then as catalyst in the HTL process which increases yield and quality of bio-

crude while depositing the MNPs in the solid residue. The MNPs can then easily be recovered and reused in the process. Thus, producing a truly sustainable process culminating in the cost-effective processing of microalgae for biofuel production via the HTL route, potentially enabling a far more efficient route to algal biofuels.

More work is still underway in our group to develop new ferrite catalysts for more efficient de-oxygenation and de-nitrogenation of bio-crude oils.

ASSOCIATED CONTENT

Supporting Information

A list of materials used, methods employed to synthesize magnetic nanoparticles, magnetic separation procedure, procedure for microalgae HTL, bio-crude analysis, TEM images of magnetite, Zn and Mg doped ferrite MNPs, XRD and UV-Vis spectrum of MNPs, graphs of particle size distribution of MNPs, graph of ζ -potential of magnetite and microalgae at different pH, table of elemental composition, HHV and ER of bio-crude synthesised with and without MNPs. Table showing the % relative area of major compounds identified from GC-MS spectrum of bio-crudes from catalysed and un-catalysed *S. obliquus* and *Spirulina* liquefaction, GC-MS spectrum of bio-crudes from *S. obliquus* and *Spirulina* liquefaction, graph of grouped compounds from GC-MS spectra of *S. obliquus*, ¹H NMR spectrum of bio-crudes from catalysed and un-catalysed *Spirulina* liquefaction, SEM images of microalgae with MNPs attached, pictorial illustration of magnetic separation process, diagrammatic illustration of a potential HTL bio-refinery applying and recycling MNPs, and a graph of bio-crude yield using recycled MNPs.

AUTHOR INFORMATION

Corresponding Author

E-mail: P.Plucinski@bath.ac.uk. Phone: +441225786961

Present Addresses

Pawel Plucinski, Department of Chemical Engineering, University of Bath. UK. Postcode: BA2 7AY

Notes

The authors declare no competing financial interests.

ACKNOWLEDGMENT

Financial support for this research was from the Commonwealth Scholarship Commission UK in form of full Scholarship funding for PhD study of Daniel Egesa.

REFERENCES

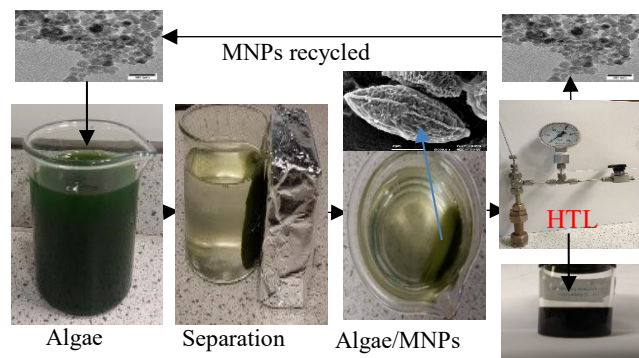
1. Chen, Y.; Zhao, N.; Wu, Y.; Wu, K.; Wu, X.; Liu, J.; Yang, M., Distributions of organic compounds to the products from hydrothermal liquefaction of microalgae. *Environmental Progress & Sustainable Energy* **2016**, DOI: 10.1002/ep.12490.
2. Duan, P.; Savage, P. E., Hydrothermal liquefaction of a microalga with heterogeneous catalysts. *Industrial & Engineering Chemistry Research* **2010**, *50* (1), DOI: 52-61. 10.1021/ie100758s.
3. Amaro, H. M.; Guedes, A. C.; Malcata, F. X., Advances and perspectives in using microalgae to produce

biodiesel. *Applied Energy* **2011**, *88* (10), 3402-3410. DOI: 10.1016/j.apenergy.2010.12.014.

4. Barros, A. I.; Gonçalves, A. L.; Simões, M.; Pires, J. C., Harvesting techniques applied to microalgae: A review. *Renewable and Sustainable Energy Reviews* **2015**, *41*, 1489-1500. DOI: 10.1016/j.rser.2014.09.037.
5. Mata, T. M.; Martins, A. A.; Caetano, N. S., Microalgae for biodiesel production and other applications: a review. *Renewable and sustainable energy reviews* **2010**, *14* (1), 217-232. DOI: 10.1016/j.rser.2009.07.020.
6. Safarik, I.; Prochazkova, G.; Pospiskova, K.; Branyik, T., Magnetically modified microalgae and their applications. *Critical reviews in biotechnology* **2015**, 1-11. DOI: 10.3109/07388551.2015.1064085.
7. Grima, E. M.; Belarbi, E.-H.; Fernández, F. A.; Medina, A. R.; Chisti, Y., Recovery of microalgal biomass and metabolites: process options and economics. *Biotechnology advances* **2003**, *20* (7), 491-515. DOI: 10.1016/S0734-9750(02)00050-2.
8. Uduman, N.; Qi, Y.; Danquah, M. K.; Forde, G. M.; Hoadley, A., Dewatering of microalgal cultures: a major bottleneck to algae-based fuels. *Journal of renewable and sustainable energy* **2010**, *2* (1), 012701. DOI: 10.1063/1.3294480.
9. Prochazkova, G.; Safarik, I.; Branyik, T., Harvesting microalgae with microwave synthesized magnetic microparticles. *Bioresource Technology* **2013**, *130*, 472-477. DOI: 10.1016/j.biortech.2012.12.060.
10. Xu, Y., et al. (2017). "Cost-effectiveness Analysis on Magnetic Harvesting of Algal Cells." *Materials Today: Proceedings* **4**(1): 50-56. DOI: 10.1016/j.matpr.2017.01.192.
11. Wang, S.-K., et al. (2015). "Harvesting microalgae by magnetic separation: A review." *Algal Research* **9** (Supplement C): 178-185. DOI: 10.1016/j.algal.2015.03.005
12. <http://www.lanl.gov/about/awards-achievements/rd100/2012.php> accessed on October 25th, 2017.
13. Rojas-Pérez, A.; Diaz-Diestra, D.; Frias-Flores, C. B.; Beltran-Huarac, J.; Das, K.; Weiner, B. R.; Morell, G.; Díaz-Vázquez, L. M., Catalytic effect of ultrananocrystalline Fe₃O₄ on algal bio-crude production via HTL process. *Nanoscale* **2015**, *7* (42), 17664-17671. DOI: 10.1039/C5NR04404A.
14. Lee, A.; Lewis, D.; Kalaitzidis, T.; Ashman, P., Technical issues in the large-scale hydrothermal liquefaction of microalgal biomass to biocrude. *Current opinion in biotechnology* **2016**, *38*, 85-89. DOI: 10.1016/j.copbio.2016.01.004.
15. Faeth, J. L.; Savage, P. E., Effects of processing conditions on biocrude yields from fast hydrothermal liquefaction of microalgae. *Bioresource technology* **2016**, *206*, 290-293. DOI: 10.1016/j.biortech.2016.01.115.
16. Zhou, D.; Zhang, L.; Zhang, S.; Fu, H.; Chen, J., Hydrothermal liquefaction of macroalgae *Enteromorpha prolifera* to bio-oil. *Energy & Fuels* **2010**, *24* (7), 4054-4061. DOI: 10.1021/ef100151h.

17. Akia, M.; Yazdani, F.; Motae, E.; Han, D.; Arandiyan, H., A review on conversion of biomass to biofuel by nanocatalysts. *Biofuel Research Journal* **2014**, *1* (1), 16-25. DOI: 10.18331/BRJ2015.1.1.5.
18. Laska, U.; Frost, C. G.; Price, G. J.; Plucinski, P. K., Easy-separable magnetic nanoparticle-supported Pd catalysts: Kinetics, stability and catalyst re-use. *Journal of Catalysis* **2009**, *268* (2), 318-328. DOI: 10.1016/j.jcat.2009.10.001.
19. Lv, Z.; Wang, Q.; Bin, Y.; Huang, L.; Zhang, R.; Zhang, P.; Matsuo, M., Magnetic Behaviors of Mg-and Zn-Doped Fe₃O₄ Nanoparticles Estimated in Terms of Crystal Domain Size, Dielectric Response, and Application of Fe₃O₄/Carbon Nanotube Composites to Anodes for Lithium Ion Batteries. *The Journal of Physical Chemistry C* **2015**, *119* (46), 26128-26142. DOI: 10.1021/acs.jpcc.5b07580.
20. Prochazkova, G.; Podolova, N.; Safarik, I.; Zachleder, V.; Branyik, T., Physicochemical approach to freshwater microalgae harvesting with magnetic particles. *Colloids and Surfaces B: Biointerfaces* **2013**, *112*, 213-218. DOI: 10.1016/j.colsurfb.2013.07.053.
21. Coma, M.; Hernandez, E. M.; Abeln, F.; Raikova, S.; Donnelly, J.; Arnot, T. C.; Allen, M.; Hong, D. D.; Chuck, C. J., Organic waste as a sustainable feedstock for platform chemicals. *Faraday Discussions* **2017**, *202*, 175-195. DOI: 10.1039/C7FD00070G
22. Neveux, N.; Yuen, A.; Jazrawi, C.; Magnusson, M.; Haynes, B.; Masters, A.; Montoya, A.; Paul, N.; Maschmeyer, T.; De Nys, R., Biocrude yield and productivity from the hydrothermal liquefaction of marine and freshwater green macroalgae. *Bioresource technology* **2014**, *155*, 334-341. DOI: 10.1016/j.biortech.2013.12.083.
23. Kaur, M.; Jain, P.; Singh, M., Studies on structural and magnetic properties of ternary cobalt magnesium zinc (CMZ) Co 0.6-x Mg x Zn 0.4 Fe₂O₄ (x= 0.0, 0.2, 0.4, 0.6) ferrite nanoparticles. *Materials Chemistry and Physics* **2015**, *162*, 332-339. DOI: 10.1016/j.matchemphys.2015.05.075.
24. Hariani, P. L.; Faizal, M.; Setiabudidaya, D., Synthesis and properties of Fe₃O₄ nanoparticles by co-precipitation method to removal procion dye. *International Journal of Environmental Science and Development* **2013**, *4* (3), 336. DOI: 10.7763/IJESD.2013.V4.366.
25. Melo, A. F.; Luz, R. A.; Iost, R. M.; Nantes, I. L.; Crespilho, F. N., Highly stable magnetite modified with chitosan, ferrocene and enzyme for application in magneto-switchable bioelectrocatalysis. *Journal of the Brazilian Chemical Society* **2013**, *24* (2), 285-294. DOI: 10.5935/0103-5053.20130037.
26. Cerff, M.; Morweiser, M.; Dillschneider, R.; Michel, A.; Menzel, K.; Posten, C., Harvesting fresh water and marine algae by magnetic separation: screening of separation parameters and high gradient magnetic filtration. *Bioresource technology* **2012**, *118*, 289-295. DOI: 10.1016/j.biortech.2012.05.020.
27. Xu, L.; Guo, C.; Wang, F.; Zheng, S.; Liu, C.-Z., A simple and rapid harvesting method for microalgae by in situ magnetic separation. *Bioresource Technology* **2011**, *102* (21), 10047-10051. DOI: 10.1016/j.biortech.2011.08.021.
28. Parks, G. A., The isoelectric points of solid oxides, solid hydroxides, and aqueous hydroxo complex systems. *Chemical Reviews* **1965**, *65* (2), 177-198. DOI: 10.1021/cr60234a002.
29. Bos, R.; Van der Mei, H. C.; Busscher, H. J., Physico-chemistry of initial microbial adhesive interactions—its mechanisms and methods for study. *FEMS microbiology reviews* **1999**, *23* (2), 179-230. DOI: 10.1111/j.1574-6976.1999.tb00396.x.
30. Dadyburjor, D. B.; Stewart, W.; Stiller, A.; Stinespring, C.; Wann, J.-P.; Zondlo, J., Disproportionated ferric sulfide catalysts for coal liquefaction: Iron-based catalysts for coal liquefaction. *Energy & fuels* **1994**, *8* (1), 19-24. DOI: 10.1021/ef00043a003.
31. Raikova, S.; Smith-Baedorf, H.; Bransgrove, R.; Barlow, O.; Santomauro, F.; Wagner, J. L.; Allen, M. J.; Bryan, C. G.; Sapsford, D.; Chuck, C. J., Assessing hydrothermal liquefaction for the production of bio-oil and enhanced metal recovery from microalgae cultivated on acid mine drainage. *Fuel Processing Technology* **2016**, *142*, 219-227. DOI: 10.1016/j.fuproc.2015.10.017.
32. Shakya, R.; Whelen, J.; Adhikari, S.; Mahadevan, R.; Neupane, S., Effect of temperature and Na₂CO₃ catalyst on hydrothermal liquefaction of algae. *Algal Research* **2015**, *12*, 80-90. DOI: 10.1016/j.algal.2015.08.006.
33. Ross, A.; Biller, P.; Kubacki, M.; Li, H.; Lea-Langton, A.; Jones, J., Hydrothermal processing of microalgae using alkali and organic acids. *Fuel* **2010**, *89* (9), 2234-2243. DOI: 10.1016/j.fuel.2010.01.025.
34. Toor, S. S.; Rosendahl, L.; Rudolf, A., Hydrothermal liquefaction of biomass: a review of subcritical water technologies. *Energy* **2011**, *36* (5), 2328-2342. DOI: 10.1016/j.energy.2011.03.013.
35. Barreiro, D. L.; Samori, C.; Terranella, G.; Hornung, U.; Kruse, A.; Prins, W., Assessing microalgae biorefinery routes for the production of biofuels via hydrothermal liquefaction. *Bioresource technology* **2014**, *174*, 256-265. DOI: 10.1016/j.biortech.2014.10.031.
36. Srokol, Z.; Bouche, A.-G.; van Estrik, A.; Strik, R. C.; Maschmeyer, T.; Peters, J. A., Hydrothermal upgrading of biomass to biofuel; studies on some monosaccharide model compounds. *Carbohydrate Research* **2004**, *339* (10), 1717-1726. DOI: 10.1016/j.carres.2004.04.018.

TOC/Abstract for Table of Content Use Only



Synopsis: Recycling MNPs for microalgae separation and HTL minimizes waste accumulation leading to a sustainable, economical, optimal and environmentally friendly process.
